

Unclassified

FILE COPY

83741  
1 2 cys.

Project Report

LTP-30

Experimental Observations  
of Thermal-Blooming Compensation  
Using a Deformable-Mirror System

C. A. Primmerman

D. G. Fouche

20 November 1975

Prepared for the Defense Advanced Research Projects Agency  
under Electronic Systems Division Contract F19628-76-C-0002 by

Lincoln Laboratory

MASSACHUSETTS INSTITUTE OF TECHNOLOGY

LEXINGTON, MASSACHUSETTS



Approved for public release; distribution unlimited.

Unclassified

ADA09465

# Unclassified

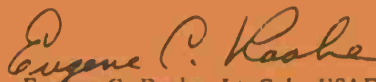
The work reported in this document was performed at Lincoln Laboratory, a center for research operated by Massachusetts Institute of Technology. This work was sponsored by the Defense Advanced Research Projects Agency under Air Force Contract F19628-76-C-0002 (ARPA Order 600).

This report may be reproduced to satisfy needs of U.S. Government agencies.

The views and conclusions contained in this document are those of the contractor and should not be interpreted as necessarily representing the official policies, either expressed or implied, of the Defense Advanced Research Projects Agency of the United States Government.

This technical report has been reviewed and is approved for publication.

FOR THE COMMANDER



Eugene C. Raabe, Lt. Col., USAF  
Chief, ESD Lincoln Laboratory Project Office

# Unclassified

Unclassified

MASSACHUSETTS INSTITUTE OF TECHNOLOGY  
LINCOLN LABORATORY

EXPERIMENTAL OBSERVATIONS  
OF THERMAL-BLOOMING COMPENSATION  
USING A DEFORMABLE-MIRROR SYSTEM

*C. A. PRIMMERMAN*

*D. G. FOUCHE*

*Group 55*

PROJECT REPORT LTP-30

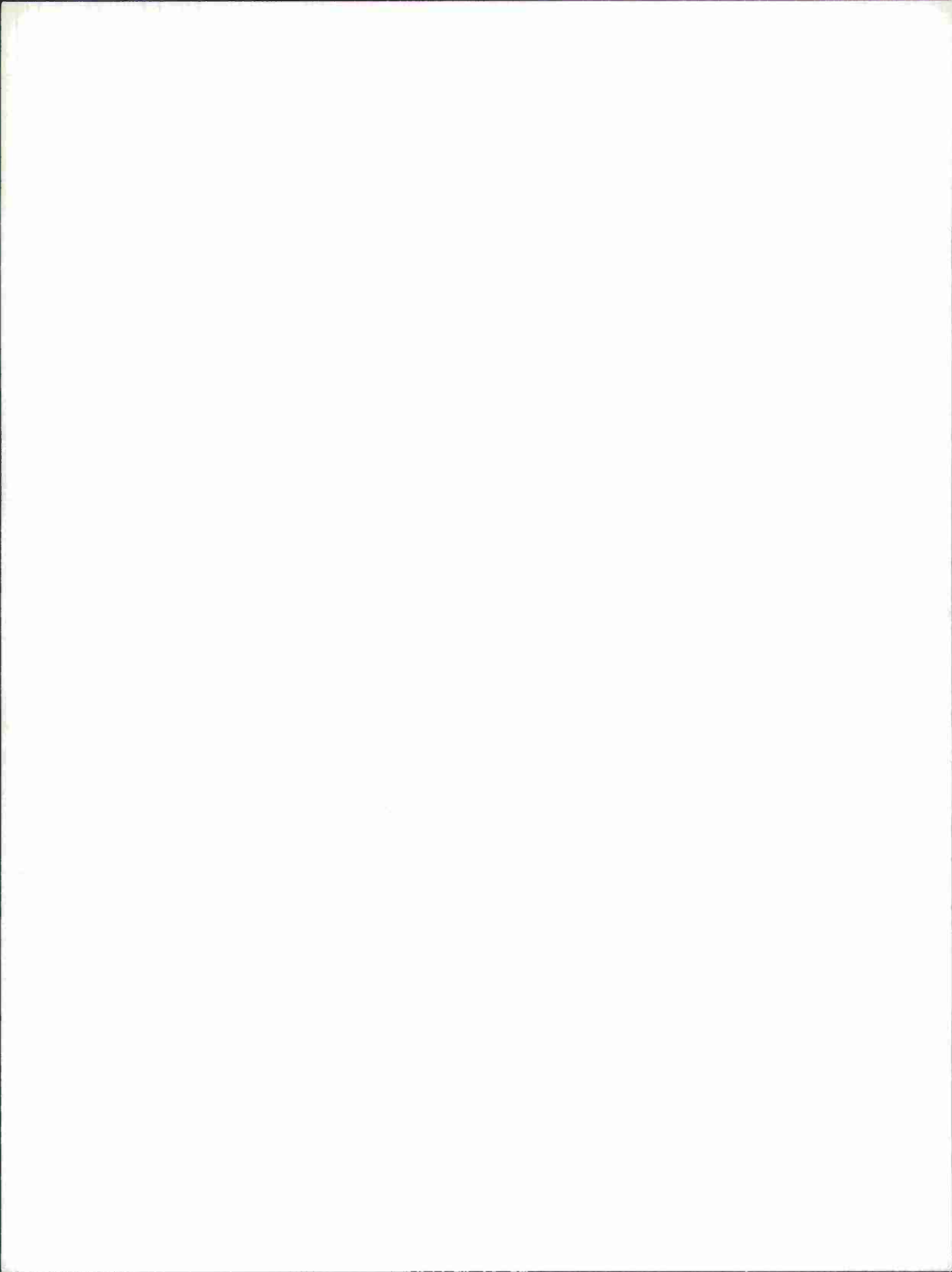
20 NOVEMBER 1975

Approved for public release; distribution unlimited.

LEXINGTON

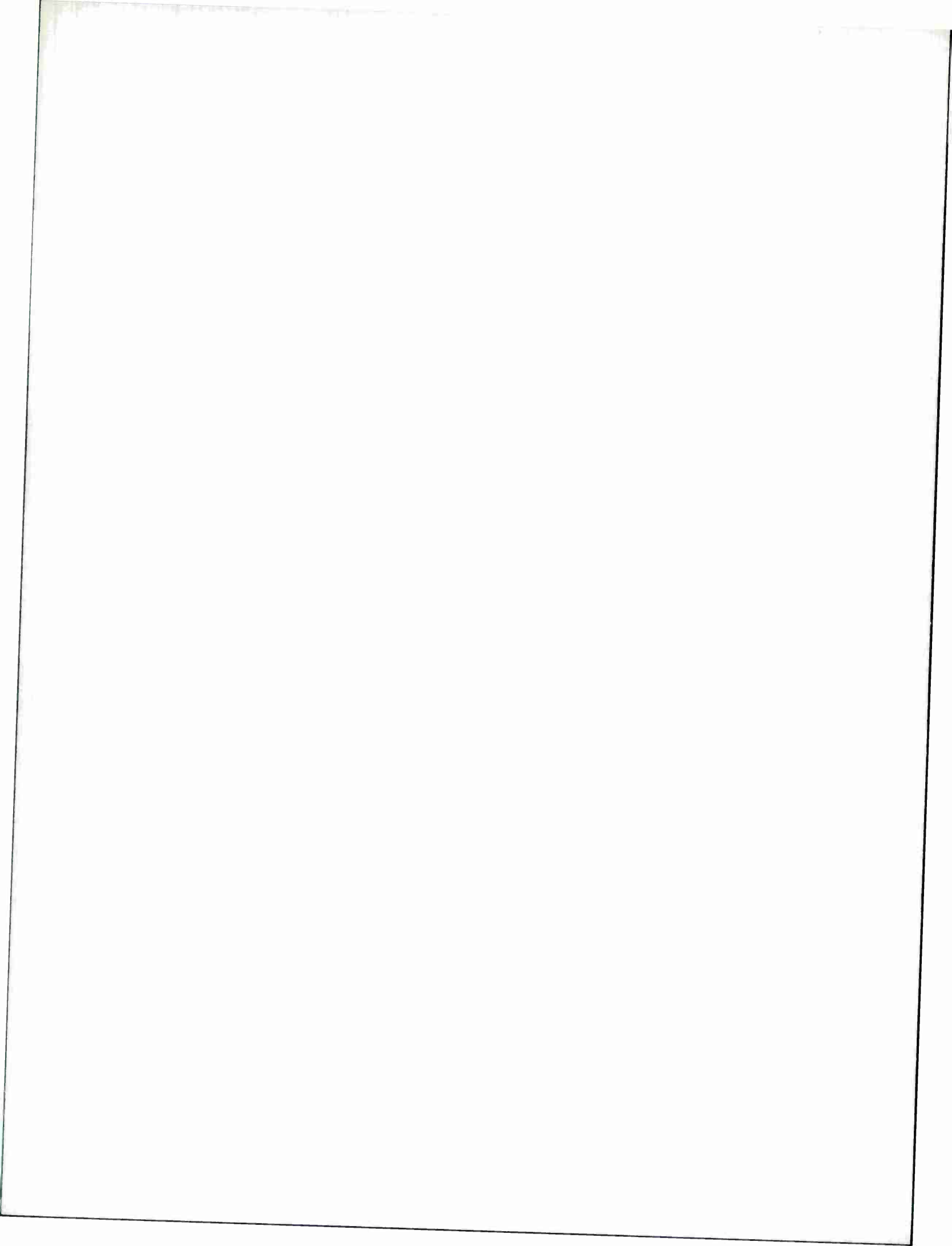
MASSACHUSETTS

Unclassified



## ABSTRACT

A laboratory experiment has demonstrated the effectiveness of compensating for forced-convection-dominated CW thermal blooming by using a deformable mirror to add phase corrections to the laser beam. In agreement with theoretical predictions, the peak focal-plane irradiance has been increased by a factor of 3 under severely bloomed conditions.



## Introduction

As a laser beam passes through an absorbing medium, it heats the medium causing the index of refraction along its path to change. The induced index of refraction gradients, in turn, cause the beam to be spread or bloomed. This phenomenon of thermal blooming severely limits the maximum focal-plane irradiance of a laser beam propagating through the atmosphere.<sup>1</sup> Recently it has been proposed that one could compensate for thermal blooming by using an adaptive-optics system to add appropriate phase corrections at the beam transmitter.<sup>2</sup> In this report we present experimental evidence conclusively demonstrating that this technique may be used to compensate for the blooming of a CW slewed laser beam. The experiment has been performed in the laboratory, but care has been taken to make all relevant propagation parameters scalable to the realistic case of a high-power laser beam propagating in the atmosphere.

## Deformable-Mirror System

We apply phase corrections to a laser beam by means of a deformable-mirror system developed by Itek Corporation.<sup>3</sup> The deformable mirror uses a novel design in that instead of having discrete actuators it consists of a monolithic disk of piezoelectric crystal into which is placed an array of electrodes. There are 57 electrodes which, energized with up to  $\pm 1500$  volts, can produce surface deformations of  $\pm 0.5$  micron over an active area 1.5 inches in diameter. The mirror surface is a metalized glass disk cemented on the piezoelectric crystal.

The electrodes may be individually actuated so that any phase profile consistent with the maximum deformation and the spatial-frequency limitation imposed by the finite number of actuators may be put on the mirror. But for the experiments reported here the relative voltages of the electrodes were

fixed by a resistive network to give the relative phase profiles shown in Fig. 1. This profile closely matches that calculated by Bradley and Herrmann<sup>2</sup> to give the maximum correction for a truncated Gaussian beam undergoing forced-convection-dominated thermal blooming, if only third-order corrections are taken into account. Thus, the profile of Fig. 1 includes third-order refocus, spherical, coma, and astigmatism terms; it does not include tilt, since tilt produces only a shift of the beam and no change in intensity. In these experiments we manually varied the amplitude of the deformation from flat to about  $2\lambda$  peak to peak but did not vary the shape.

#### Experimental Conditions

The experimental arrangement is shown in Fig. 2. We use a CW argon-ion laser that produces a Gaussian beam with up to 2 watts of useful power at  $5145 \text{ \AA}$ . The beam is expanded to make the  $1/e^2$  diameter 1.5 inches, is truncated at this diameter, and is reflected from the deformable mirror. The beam is then contracted and is slewed through the absorption cell by a variable-speed slewing mirror. In the focal plane just beyond the cell we have a row of 50-micron pinholes at a slight angle to the slewed beam. By detecting the light coming through these pinholes we can measure both the intensity and the shape of the bloomed beam as it leaves the gas cell. The optics are such that with the absorption cell empty the focal-spot diameter is within  $\sim 10\%$  of the diffraction limit.

The gas cell is filled with a few torr of  $\text{NO}_2$ , enough to absorb  $\sim 50\%$  of the incident radiation in the 1.5-m-long tank, and one atmosphere of a non-absorbing buffer gas. Since we are interested in studying the thermal blooming of a slewed beam (that is, one in which forced convection is the dominant cooling mechanism), the gas cell is mounted vertically to minimize

free-convection cooling, and  $\text{CO}_2$  is used as the buffer gas to reduce conduction cooling. Mounting the gas cell vertically effectively eliminates free-convection effects; but, unfortunately conduction effects are not always negligible and must be taken into account.

As shown by Bradley and Herrmann,<sup>2</sup> the propagation of a slewed beam through an absorbing medium can be characterized by the four dimensionless numbers:

$$\text{Absorption Number} - N_A \equiv \alpha R$$

$$\text{Fresnel Number} - N_F \equiv ka^2/R$$

$$\text{Slewing Number} - N_\omega \equiv \omega R/v$$

$$\text{Distortion Number} - N_D \equiv (1/\rho c_p \epsilon_0)(\partial \epsilon / \partial T)(\alpha P k R / av)$$

where  $\alpha$  is the absorption coefficient,  $R$  is the range,  $k$  is the wave number,  $a$  is the  $1/e$  radius at the cell entrance,  $\omega$  is the slewing frequency,  $v$  is the constant cross-wind velocity,  $P$  is the incident power, and  $(1/\rho c_p \epsilon)(\partial \epsilon / \partial T)$  is a constant characterizing the change in index of refraction of the heated gas. For our laboratory experiment an additional dimensionless number is required as a measure of the importance of conduction compared to forced convection:

$$\text{Conduction Number} - N_C \equiv \kappa / \sqrt{2} av$$

where  $\kappa$  is the thermal diffusivity.

The actual experimental conditions are given by the following set of parameters:

$$\alpha = 4.6 \times 10^{-3} \text{ cm}^{-1}$$

$$R = 150 \text{ cm}$$

$$k = 1.22 \times 10^5 \text{ cm}^{-1}$$

$$a = 0.25 \text{ cm}$$

$$\omega = 0 \text{ to } 0.2 \text{ rad/sec (variable)}$$

$$v = 0 \text{ to } 3 \text{ cm/sec (variable)}$$

$P = 0.03$  to  $1$  watt (variable)

$$(1/\rho c_p \epsilon_0)(\partial \epsilon / \partial T) = 1.95 \times 10^{-3} \text{ J}^{-1} \text{ cm}^3$$

$$\kappa = 0.11 \text{ cm}^2\text{-sec}^{-1}$$

$$N_A = 0.69$$

$$N_F = 45$$

$$N_\omega = 7.5 \text{ to } 30 \text{ (variable)}$$

$$N_D = 686 P/v \text{ (variable)}$$

$$N_C = 0.1 \text{ to } \infty \text{ (variable)}$$

The three basic variables in this experiment are the input power at the cell entrance,  $P$ , the slew frequency,  $\omega$ , and the constant cross-wind velocity,  $v$ , which can be varied independently of  $\omega$  by changing the distance from the slewing mirror to the cell entrance. These variables enable us to test the dependence of the thermal-blooming corrections on the dimensionless numbers  $N_\omega$ ,  $N_D$ ,  $N_C$ . We can also vary  $N_A$  and  $N_F$ , but in these experiments no attempt has been made to systematically study the effect of these parameters on phase correction for thermal blooming.

### Experimental Results

#### 1. Results of Varying Power

In Fig. 3 we show the measured peak focal-plane intensity plotted against input power for the uncorrected beam, the corrected beam, and the hypothetical situation of absorption with no blooming. Varying the power is equivalent to varying the distortion number, since  $N_D \propto P$ . The uncorrected curve was taken with the deformable mirror in the flat condition; the corrected curve was obtained by adjusting the amplitude of the mirror deformation to get the maximum possible intensity at each power.

The uncorrected curve exhibits the classic thermal-blooming behavior: the intensity first increases with increasing power and then, after a certain critical power,  $P_C$ , decreases with further increases in the input power. As expected, the corrected curve shifts upward to higher intensities and outward to higher critical power. We observe that the maximum intensity increases 76% over the uncorrected case and that at certain powers there is a factor of 3 increase in intensity. This result is representative: we have consistently achieved improvements in maximum intensity of ~70%. We also observe that the critical power increases by almost a factor of 2.5. For laser weapons applications, the quantity of interest is  $P_O$ , the total power deposited on target by that part of the beam having intensity above some threshold intensity,  $I_O$ . For a fixed beam profile,  $P_O$  is a function of the input power,  $P$ , and the ratio of the peak intensity to the threshold intensity,  $I_p/I_O$ . Thus, a reasonable figure of merit in atmospheric propagation is  $I_p(P_C)P_C$ , the maximum intensity times the critical power. On the basis of this figure of merit we have achieved a four-fold improvement in laser effectiveness using our deformable-mirror system.

Figure 4 shows oscilloscope traces of the detector voltage as the beam sweeps across our pinhole array. The lower trace shows the severely bloomed beam at  $P = 0.45$  watt; the upper trace shows the corrected beam at the same power. We see that the peak intensity has increased by almost a factor of 3 and that the beam shape has been greatly improved.

Figure 5 shows actual photographs of the beam in the focal plane. In the top picture we see the characteristic crescent-shaped bloomed beam. In the next picture we see the corrected beam, reduced in size and with only a slight remaining indication of a crescent shape. For comparison, the bottom photograph shows the low-power unbloomed beam. (The somewhat elliptical shape results

from the fact that the shutter speed is not fast enough to "freeze" the beam.) Note that the corrected and uncorrected bloomed beams are both shifted into the wind with respect to the unbloomed beam, since our deformable mirror does not add a tilt correction. We observe that, consistent with the intensities shown in Fig. 3, the corrected spot size is still larger than the unbloomed spot size.

## 2. Comparison with Propagation-Code Results

To compare our experimental results with the theoretical predictions for phase compensation of thermal blooming we have employed the Bradley-Herrmann propagation code. In Fig. 6 we show propagation-code-generated plots of peak focal-plane irradiance against power for no correction and for two different corrections. The upper corrected curve is the optimum correction using the Bradley-Herrmann method; the lower corrected curve is the correction obtained using the Zernike polynomial expansion of the contour actually on the mirror. The input parameters used in the code were the experimentally measured conditions corresponding to the results of Fig. 3. To facilitate comparison of theory and experiment the curves of Figs. 3 and 6 have been normalized to the same unbloomed intensity.

Looking first at the uncorrected curves we note that both theoretical and experimental curves follow roughly the dependence  $I_p \propto P \exp(-P/P_c)$  until  $P \approx 2P_c$ . Beyond this point the curves fall off much more slowly than given by the exponential dependence. At  $P = 3P_c$ , for instance, the theoretical curve has a peak irradiance twice that given by the simple exponential dependence. The theoretical curve peaks at  $P = 0.155$  watts; the experimental curve, at  $P = 0.18$  watt. Thus, the critical powers agree to within ~15%--good agreement considering the many possibilities for consistent error. But although the critical powers agree well, the experimental and theoretical maximum intensities

are not in such good agreement. Some of the disagreement is attributable to the difference in  $P_C$ . But, as illustrated in Fig. 3, we often find that the experimentally determined intensity at  $P_C$  is about 1/2 the unbloomed intensity, while the theoretical prediction is that the intensity at  $P_C$  should be 1/e times the unbloomed intensity. The reason for this disagreement is still unclear.

Comparing the corrected curves we find that the experimental curve falls almost on the optimum theoretical curve; but this agreement is probably a fortuitous coincidence resulting from the consistent shift between theoretical and experimental results. To more properly compare the corrected curves we refer to Table I and compare the increases in irradiance over the uncorrected values. Experimentally we observe that the maximum intensity increases a factor of 1.76 compared to 1.98 for the theoretical increase --an agreement within 15%. The maximum increase at any power is 2.87 experimentally compared to 2.48 theoretically --again an agreement within 15%. The agreement in  $P_C$  is not so close --2.44 experimentally to 1.94 theoretically --but a look at Fig. 3 shows that it is extremely difficult to determine accurately the critical power for the experimental corrected curve.

The experimental correction is still ~ 30% below the optimum correction. This difference results primarily not from any deficiency of the mirror but from the fact that only third-order corrections were specified for the mirror surface. Theoretically, adding phase corrections through fifth order results in corrected intensities very close to optimum; so there is reason to believe that if the mirror figure were corrected through fifth order the experimental curve would also approach the optimum.

The propagation-code results are seen to give quantitative agreement with the experimental results to within about 15%. Considering the many

TABLE I

	$P_C$	$I_p(P_C)$	$\frac{P_C \text{ (corrected)}}{P_C \text{ (uncorrected)}}$	$\frac{I_p(P_C) \text{ corrected}}{I_p(P_C) \text{ uncorrected}}$	Max $\frac{I_p \text{ corrected}}{I_p \text{ uncorrected}}$
Experimental Uncorrected	0.18	0.90	--	--	--
Experimental Corrected	0.44	1.55	2.44	1.76	2.87
Theoretical Uncorrected	0.155	0.56	--	--	--
Theoretical Mirror Corrected	0.300	1.11	1.94	1.98	2.48
Theoretical Optimum Corrected	0.415	1.53	2.68	2.73	4.33

parameters involved in making the comparison --eleven experimental values must be supplied in the propagation code --and the concomitant chances for consistent error we believe this 15% agreement represents very good agreement indeed.

### 3. Results of Varying Cross-Wind Velocity

In our experimental arrangement we can vary the effective cross-wind velocity,  $v$ , while keeping  $N_\omega$  constant, by varying the slew frequency,  $\omega$ . In the absence of conduction the cross-wind velocity and the input power appear only in the distortion number and only in the combination  $N_D \propto P/v$ . Thus, we expect that the critical power,  $P_C$ , and the maximum intensity,  $I_p(P_C)$ , should increase linearly with  $v$ . Experimental results verify this expectation. If  $v$  is large enough to make conduction negligible,  $P_C$  and  $I_p(P_C)$  are proportional to  $v$  for both uncorrected and corrected beams.

Since  $N_C \propto 1/v$ , as  $v$  becomes small, conduction becomes important and this linear behavior is no longer observed. And as  $v \rightarrow 0$ , conduction dominates, and  $P_C$  and  $I_p(P_C)$  approach constant values determined by conduction alone. In addition, as conduction becomes important, our phase corrections become less effective, since the phase profile was derived using a theoretical treatment that neglected conduction. This effect may be seen in Fig. 7, where we plot the percentage increase in  $I_p(P_C)$  against  $1/N_C$ . When  $1/N_C = 0$ , conduction is the only cooling mechanism and no correction is obtained. As  $1/N_C$  increases, forced-convection cooling becomes more effective and the percentage improvement rises sharply. Finally, when  $1/N_C$  reaches a value such that conduction is negligible compared to forced convection, the improvement levels off at its maximum value. From these results we conclude that if  $N_C \lesssim 0.3$ , conduction may be ignored compared to forced convection.

#### 4. Results of Varying Slewing Number

By simultaneously changing the distance from the slewing mirror to the cell entrance and adjusting  $\omega$ , we can change  $N_\omega$  while keeping  $v$  constant. Increasing  $N_\omega$  increases the cooling at the far end of the cell relative to that at the cell entrance; thus, as  $N_\omega$  increases, the region over which significant blooming occurs is compressed towards the cell entrance. This compression of the blooming zone should, in turn, make it easier for adaptive optics systems to correct for the blooming.

The experimental results are shown in Fig. 8, where we plot percentage increase in maximum intensity against  $N_\omega$ . We observe that, consistent with theoretical predictions, the phase correction is more effective at higher slewing numbers. At first, the percentage improvement increases roughly linearly with  $N_\omega$ , but as  $N_\omega$  is further increased the incremental improvement decreases. Thus, there is some indication that a practical limit may be reached beyond which further reducing the blooming zone does not significantly improve the correction.

#### 5. Required Accuracy of Phase Correction

In Fig. 3 we showed a corrected curve with the mirror amplitude always adjusted to give maximum intensity. But from a practical point of view, it is also important to know how sensitive this maximum is to changes in the deformation amplitude. In Fig. 9 we plot peak irradiance against peak-to-peak mirror deformation for a particular set of experimental conditions.  $I_p$  is normalized so that  $I_p = 1.0$  when the deformation is zero (mirror flat); the shape of the mirror contour is still given by Fig. 1. We note that the peak corrected intensity is a factor of 2.5 greater than uncorrected--a respectable correction. But equally important, we observe that the correction curve is

bell-shaped with an extremely broad peak. The width at 90% maximum is marked; we see that the amplitude of the phase correction can vary  $\pm 30\%$ , while the irradiance decreases only 10%. This result is extremely encouraging, for it demonstrates that one does not have to apply phase corrections with great precision for them to be effective.

Our experimental results are uniformly in accord with the case shown. In each case there is a broad maximum in the irradiance vs. deformation curve. This pleasant result was unanticipated theoretically, but we have since checked our results using the Bradley-Herrmann propagation code. We found theoretically that varying the deformation amplitude  $\pm 20\%$  from optimum produced only a 5% decrease in peak intensity -- a result in good agreement with the experimental results.

### Conclusions

In this investigation we have obtained the first experimental evidence for the feasibility of compensating for CW convection-dominated thermal blooming by using a deformable-mirror system to add phase corrections to the laser beam. Based on our results we draw three conclusions:

1. The technique of phase compensation works. We have conclusively demonstrated that this technique can produce significant increases in transmitted intensity in a laboratory experiment. And since our laboratory experiment has been carefully scaled to model the propagation of high-power beams in the atmosphere, we conclude that phase compensation should work for these laser beams as well. Further work is necessary to determine the operational limits of the correction method, but the basic applicability has now been experimentally proven.

2. The Bradley-Herrmann propagation code accurately predicts the effects of phase compensation. Our experiment has provided the first detailed comparison of propagation-code and experimental results for phase-compensated beams. The generally good agreement between experimental and theoretical results has verified the ability of the propagation code to predict effects of phase compensation. Thus, we conclude that the code can be used with confidence to predict the characteristics of phase compensation for high-power laser beams propagating in the atmosphere.

3. The relative insensitivity of the correction to the precise amplitude of the mirror deformation offers encouragement for a practical system. In fact, this lack of sensitivity creates the interesting possibility that a predictive phase-compensation system, with perhaps several selectable phase profiles and an amplitude control, may be an attractive alternative to the far more complicated full multi-dither system.

#### ACKNOWLEDGMENTS

We thank J. Herrmann and L. A. Popper for help with the propagation code and J. J. Tynan for help with the experimental apparatus.

#### REFERENCES

1. See, for example, F. G. Gebhardt and D. C. Smith, IEEE J. Quantum Electron. QE-7, 63 (1971), and A. H. Aitken, J. N. Hayes, and P. B. Ulrich, Appl. Opt. 12, 193 (1973).
2. L. C. Bradley and J. Herrmann, Appl. Opt. 13, 331 (1974), DDC AD-785088/6.
3. J. Feinlieb, S. G. Lipson, and P. F. Cone, Appl. Phys. Lett. 25, 311 (1974).

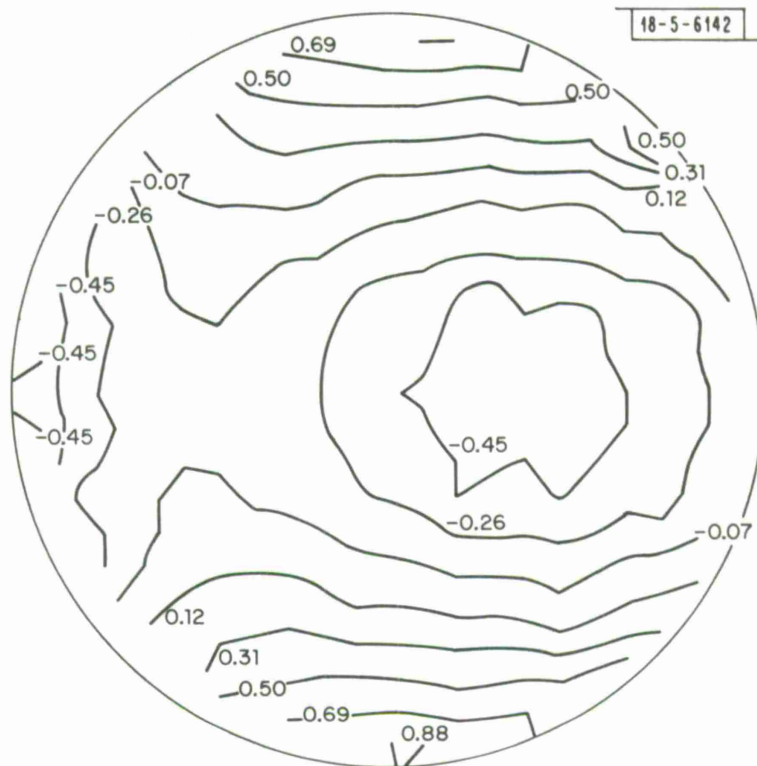


Fig. 1. Surface contour on the deformable mirror. The profile was determined by computational analysis of the laser-beam propagation. Contours are labelled in units of wavelength.

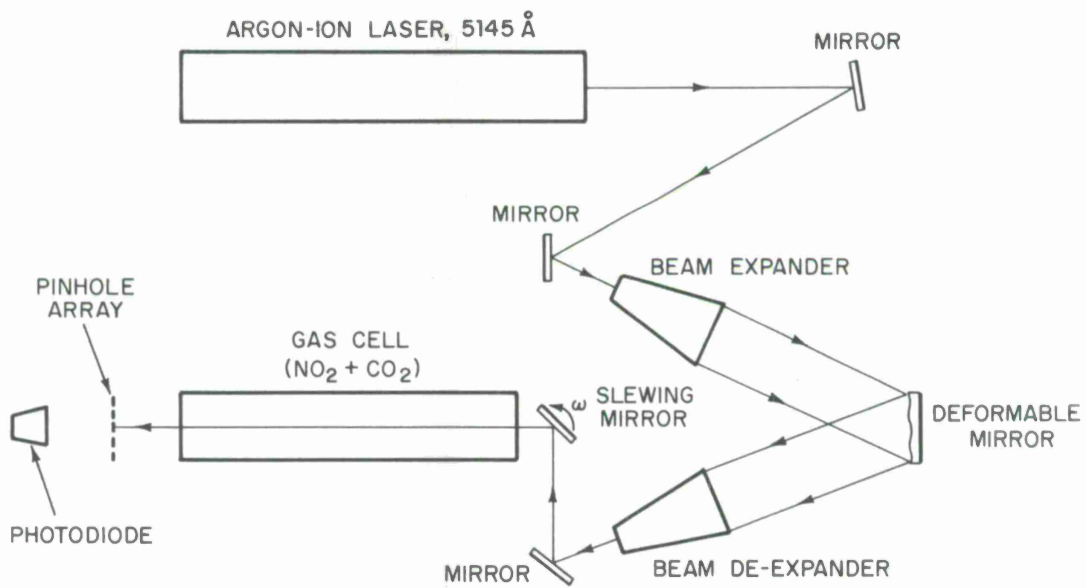


Fig. 2. Experimental arrangement

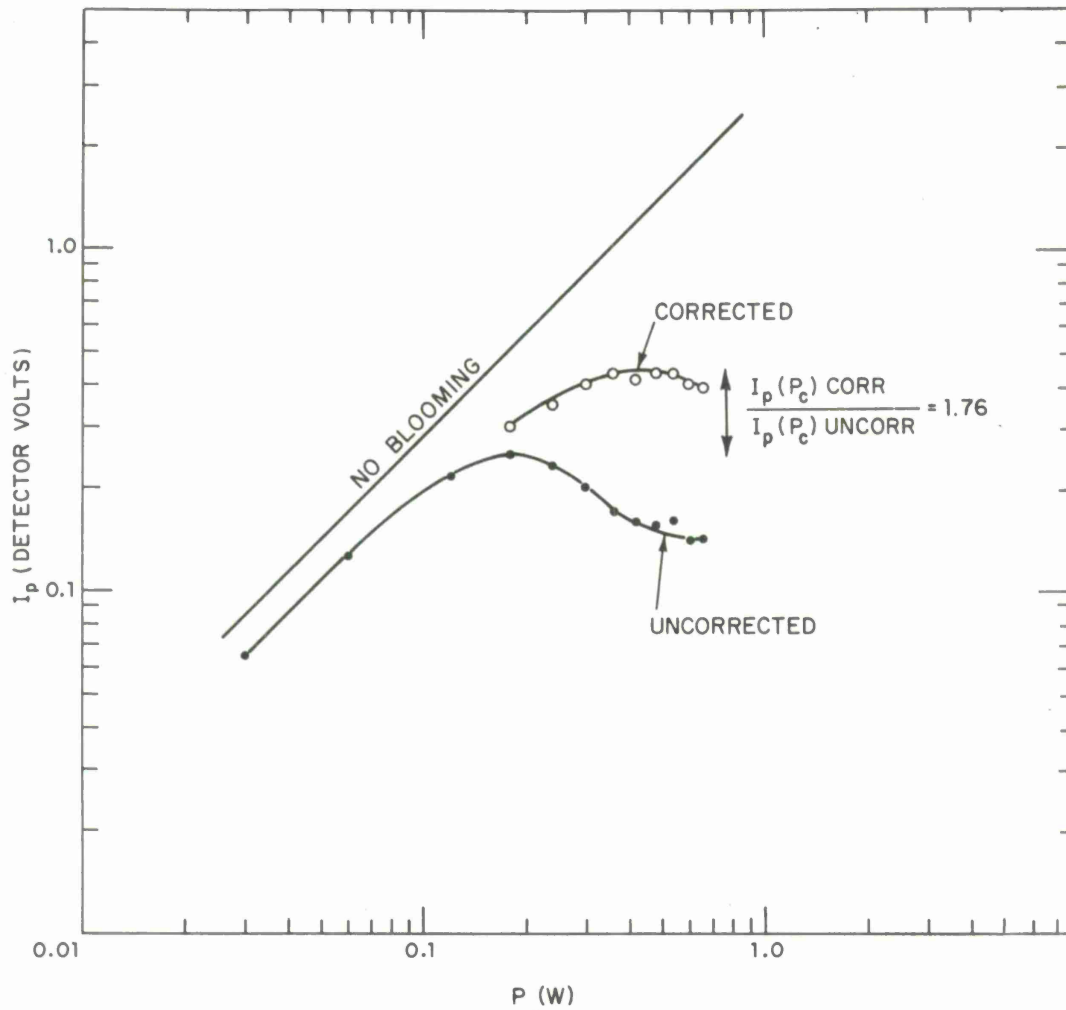


Fig. 3. Peak focal-plane intensity vs. input power for corrected and uncorrected beams. The straight line would be the intensity if there were absorption but no blooming.  $v = 1.65$  cm/sec,  $N_C = 0.19$ ,  $N_\omega = 10$ . Other parameters are listed in the text.

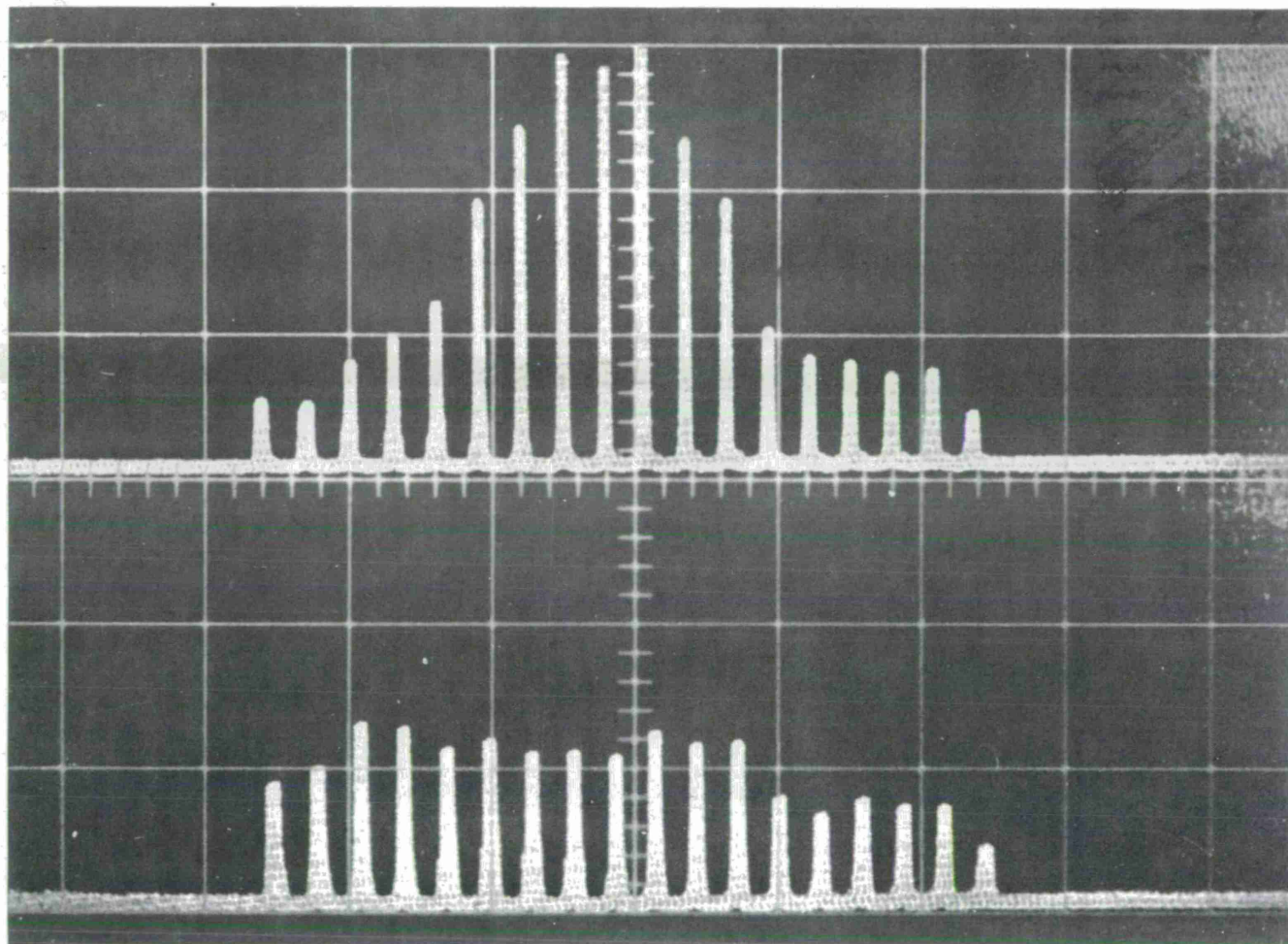
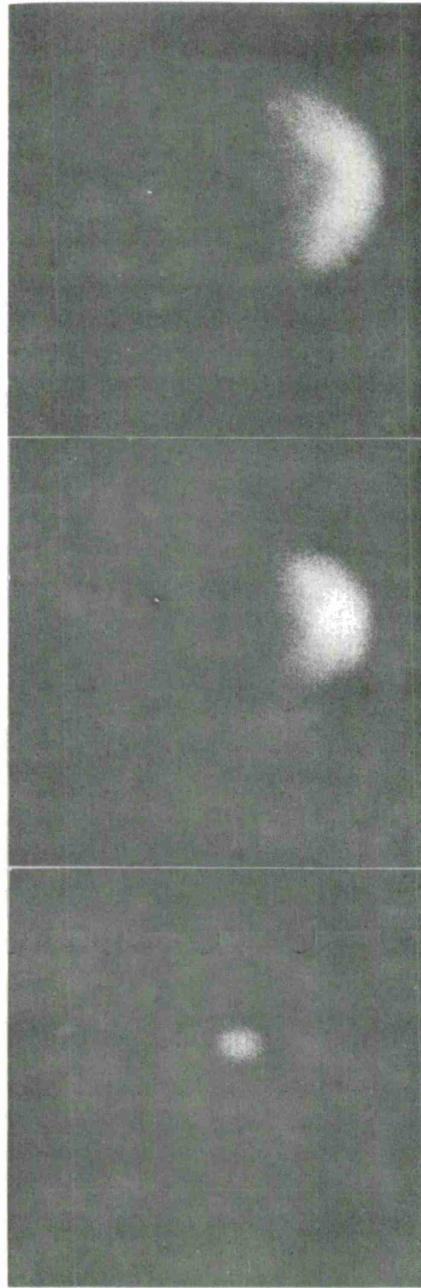


Fig. 4. Intensity through pinhole array for severely bloomed conditions at  $P = 0.45$  watts. Lower curve: uncorrected. Upper curve: corrected. Parameters as in Fig. 3.

-5-6410-1



**HIGH POWER  
(uncorrected)**

**HIGH POWER  
(corrected)**

**LOW POWER  
(uncorrected)**

Fig. 5. Actual photographs of the bloomed, corrected, and unbloomed beams in the focal plane. The top two pictures correspond to the pinhole traces of Fig. 4. The slight ellipticity of the unbloomed spot results from insufficient shutter speed to "freeze" the beam.

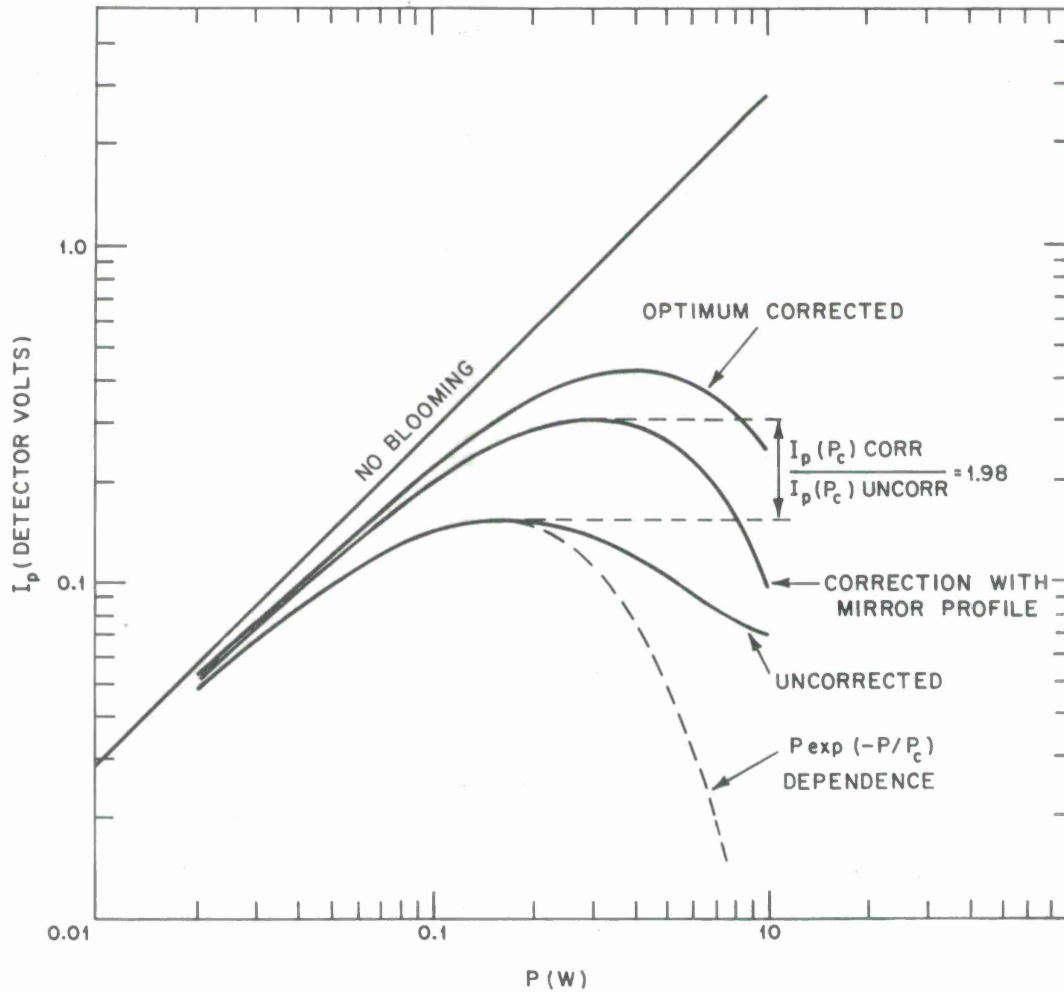


Fig. 6. Propagation-code results of peak focal-plane intensity vs. input power with and without correction. The straight line would be the intensity if there were absorption but no blooming. The dotted line represents the suggested dependence  $I_p \propto P \exp(-P/P_c)$ . Input parameters for the code were the experimental conditions of Fig. 3.

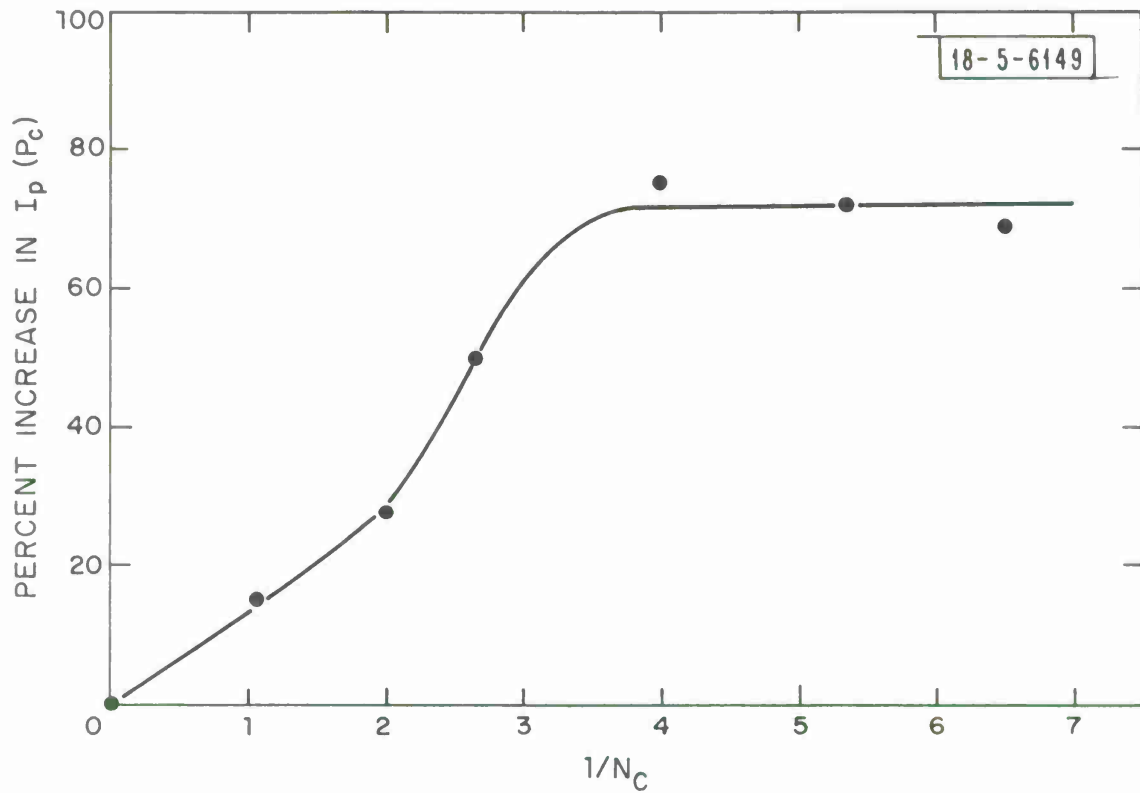


Fig. 7. Percentage increase in maximum intensity vs.  $1/N_C \cdot N_\omega = 10$ . Other parameters are listed in the text.

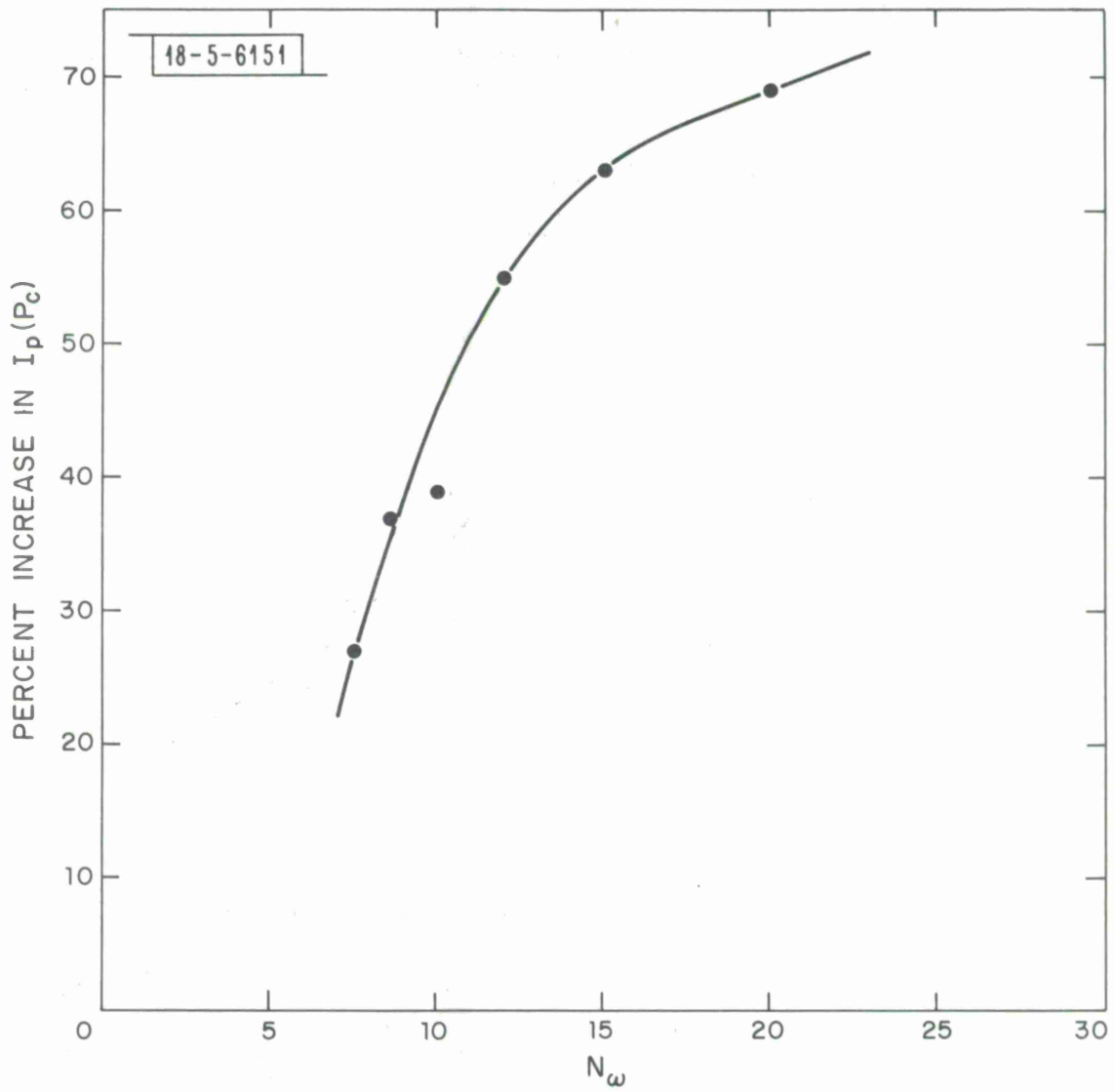


Fig. 8. Percentage increase in maximum intensity vs. slewing number.  $v = 1.65$  cm/sec,  $N_C = 0.19$ . Other parameters are listed in the text.

18-5-6373

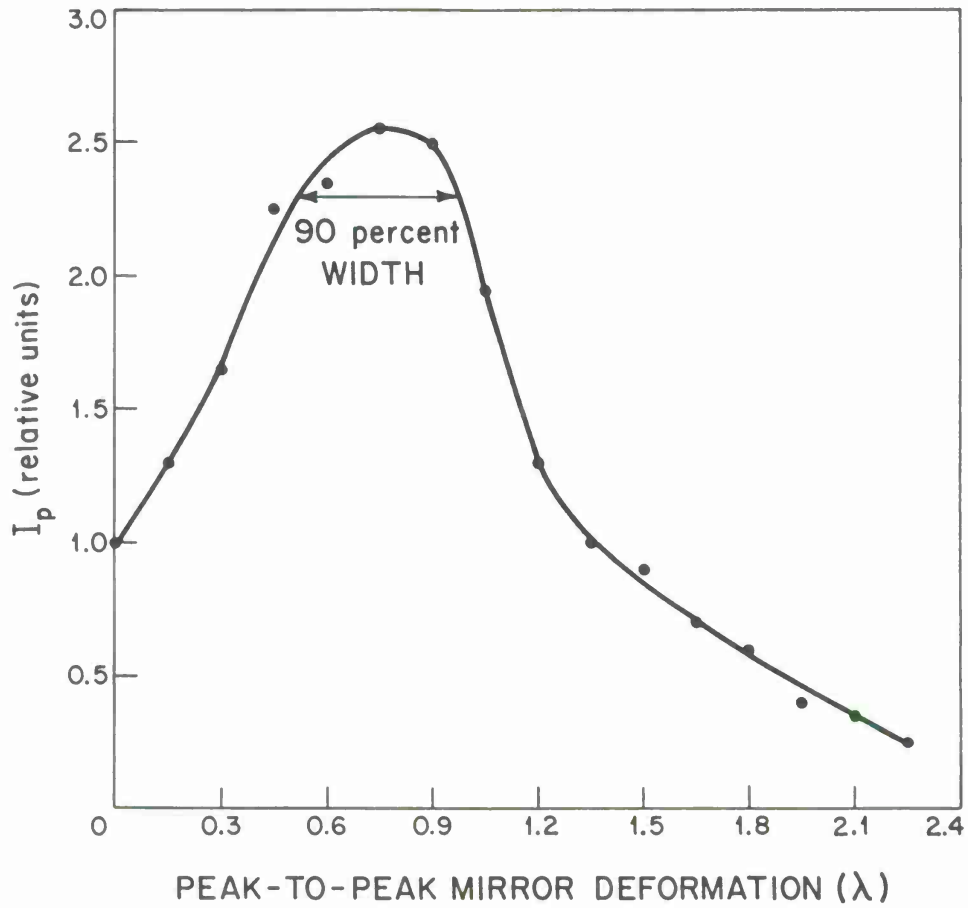


Fig. 9. Peak focal-plane intensity vs. peak-to-peak mirror deformation amplitude. The mirror profile is given in Fig. 1.  $v = 1.65$  cm/sec,  $N_C = 0.19$ ,  $N_\omega = 10$ ,  $P = 0.4$  watts. Other parameters are listed in the text.



Unclassified

Unclassified